Article

Global Megacities and Frequent Floods: Correlation between Urban Expansion Patterns and Urban Flood Hazards

Dorcas Idowu [1],* and Wendy Zhou [2]

[1] Department of Civil and Environmental Science, College of Engineering and Computer Science, Syracuse University, Syracuse, NY 13244, USA
[2] Department of Geology and Geological Engineering, Colorado School of Mines, Golden, CO 80401, USA
*   Correspondence: doidowu@syr.edu

Abstract: With climate change causing increased extreme weather events, megacities worldwide are experiencing unprecedentedly devastating floods and recurring flood damage. Investigating global megacities' increased disposition to flooding will aid in developing sustainable flood-risk-management frameworks. Many studies have been conducted on the association between land-cover types and flood consequences, but few on investigating urban expansion patterns' correlation with flood hazard and risk. This study examines the correlation between urban expansion patterns and increased flood hazards. Twelve megacities throughout the world were selected for this study. After exploring the possibility of the megacities having experienced flooding, we qualified their patterns of urban expansion and their potential to influence the elements of flood risk. Our results revealed that edge expansion and leapfrogging patterns had a strong positive correlation with statistical significance with flood hazard, while infilling had a weak positive correlation that showed no statistical significance with flood hazard. Further, we found that the megacities have all experienced devastating floods in the past two decades. Flood risk frameworks need to account for the impact of these patterns, and future urban planning designs and policies need to incorporate flood risk frameworks that account for patterns of urban expansion.

Keywords: megacity; floods; urbanization; landscape patterns; urban flood hazard; urban sustainability; change detection; land use and land cover

1. Introduction

Whether we like it or not, the global human population will continue to rise, land use and land cover will continue to change, the rain will continue to fall, and floods will not go away. With the recent events of catastrophic floods in urban and rural settings globally, it is evident that much attention is required to ameliorate the detrimental effects of flooding, especially with climate change having arrived. The authors of [1] showed that flood risk is a global threat affecting the inhabitants of 188 countries. Between 2021 and 2022 alone, there has been severe flooding in the United States, China, Japan, United Kingdom, Russia, France, Germany, Nigeria, Pakistan, India, and Bangladesh, to mention a few. These events have led to the loss of lives, properties, infrastructural damage, and grounded socioeconomic activities. Globally, it is now evident that flooding is not constrained to a geographic location but occurs in both developed countries with active flood management protocols and developing countries with sparse to no flood management. With the intensity and duration of the rainfall events leading to these floods, it is arguably evident that climate change is here.

As climate change and associated environmental impacts lead to intensifying rainfall patterns globally, many human populations globally are in the midst of a rural diaspora [2,3]. In 2007, for the first time in human history, it was estimated that more of the global population lived in urban areas than in rural areas. In 2020, the United Nations estimated that 55%

of the global population lived in cities. By 2050, it is projected that two-thirds of the global population will live in urban areas (https://datacatalog.worldbank.org/search/dataset/0037712/World-Development-Indicators, accessed on 12 November 2022). The rapid increase in urban populations will lead to a rapid expansion of urban areas, specifically in megacities or cities with a population of over 10 million [4]. As the global urban population increases, there is also an increase in urban development and expansion in land areas covered in impervious surfaces in and around global megacities, drastically increasing the surface runoff generated per unit of precipitation [5]. In most of these developed cities, rainfall events that would normally not result in environmental problems, such as flooding, now cause major catastrophes resulting in the loss of lives and properties [5–7], which is argued to be now exacerbated by climate change. Climate change and risky urbanization patterns have been investigated by researchers [1] as aggravating flood risk. Meanwhile, torrential rain events within a catchment that met with a high percentage of paved surfaces result in surface runoff that exceeds the capacity of storm drainage, resulting in flooding [8]. This type of flooding is called pluvial flooding [9], and is usually known to impact areas independent of their proximity to water bodies.

Furthermore, land use and land-cover changes involving the conversion of wetlands and/or floodplains to built-up land cover have been established to be a culprit for flooding [10]. While exposure to flooding in most parts of the world is already increasing due to climate change [1], land use and land-cover changes and expansion patterns that increase flooding exposure and risk are now more important than ever in current flood risk management and mitigation. In most flood risk modeling and vulnerability assessments, the focus is often placed on the hydrologic and hydraulic parameters of a catchment, which is an equally important approach. However, anthropogenic modifications and changes within the catchment are also known to change the characteristics or behavior of the catchment in the processing of hydrologic input. Unfortunately, these changes often increase human properties and infrastructural exposure. Han et al. [11] studied how urban expansion spatial patterns on built-up land in floodplains is a driver for flood risk and demonstrated that the pattern of urban expansion (infilling, edge expansion, and leapfrogging) influences flood vulnerability.

Several works have been undertaken on urban growth/expansion landscape patterns, and this research primarily focuses on quantifying the distribution as well as the spatiotemporal patterns associated with land use and land-cover changes on a country or city scale. Meanwhile, research establishing the type of growth mode(s) influencing environmental vulnerabilities to floods has not been fully explored. However, some recent studies [11,12] have demonstrated a link between urban expansion patterns in built-up land in floodplains (BLF) and flood exposure and vulnerability by arguing that the former dynamics (types and sizes) are key to effective understanding and management of flood risk. Meanwhile, with climate change and associated intensities in hydrologic extremes, especially torrential rainfall, it is evident that BLFs are not the only areas to consider, but that it is also important to consider built-up lands within a catchment with a sufficient number of impervious surfaces and where the location favors pluvial and flash floods. Additionally, understanding which growth modes (leapfrogging, infilling, and edge expansion) are associated with flooding would provide insight into future urban planning and into resilient flood risk strategies that would be sustainable and adaptive to current and future climate scenarios. Therefore, our study focuses on (1) estimating the patterns of expansion for twelve megacities (Figure 1), which were assumed to be urbanized because of their high population; (2) identifying which pattern is common to the cities; and (3) identifying which urban expansion pattern or growth mode is associated with increased flood hazard (Figure 2). To achieve our objectives, we assumed that a megacity with over ten million inhabitants would have experienced substantial urban developments, such that a huge amount of its landscape would have been paved, and hence be impervious. These landscape changes could cause a decrease in rainfall infiltration into the ground and favor increased runoff, which, depending on the topography and the capacity of natural/engineered drainages within the city, could

result in a flood situation. Based on these assumptions, we first proposed a question: Of the twelve megacities being studied, how many have experienced flooding in the past and when? Following this, hinging on the knowledge from answering our proposed question, we finally proceeded to the main goals of this work.
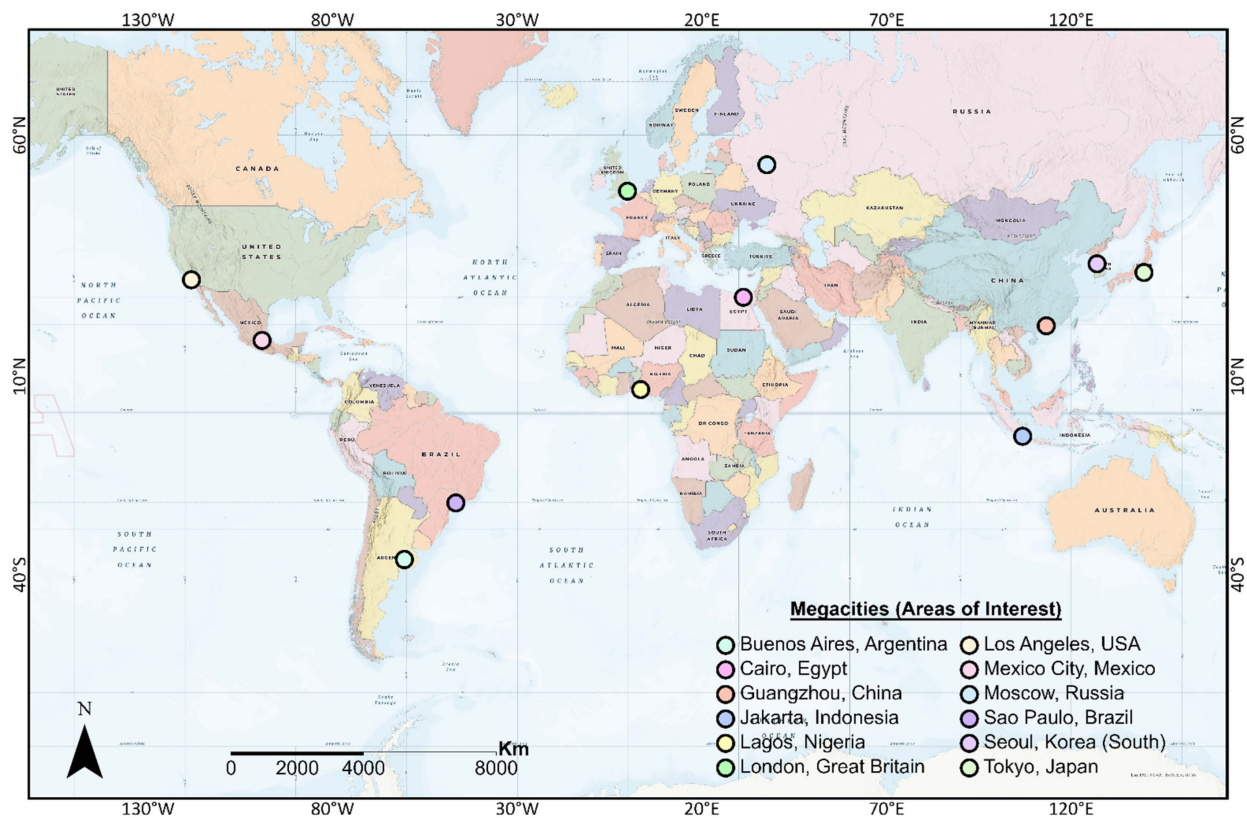

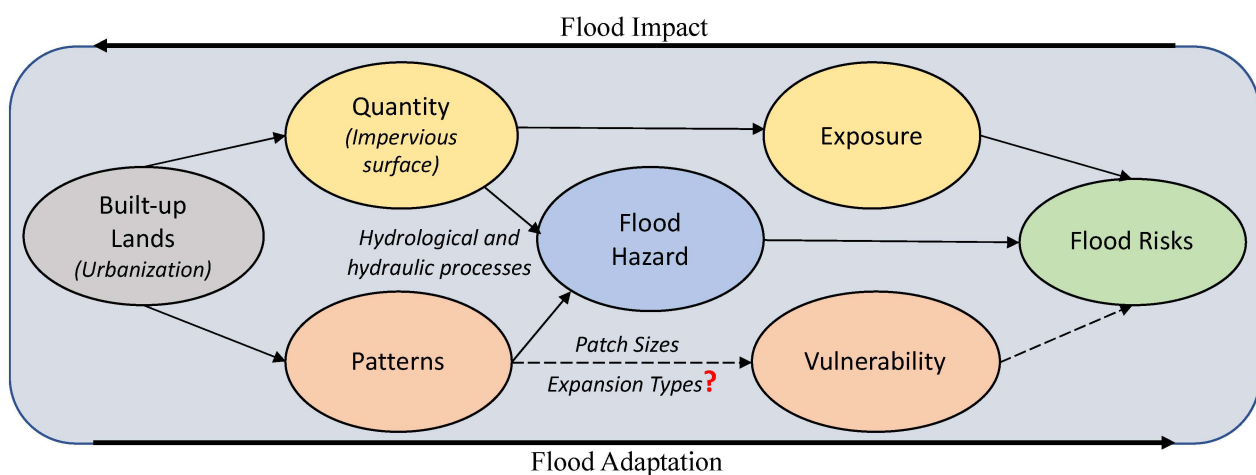**Figure 1.** Map showing the locations of megacities.

Figure 2. Impervious surfaces can influence flood risk in two ways: (1) changing flood exposure because of its changes in quantity, and (2) changing flood vulnerability due to its spatial patterns. However, the latter issue is still to be clarified. (Modified after [11]).

2. Materials and Methods

2.1. Data

2.1.1. Landsat Imagery

The Landsat scenes used for our analysis were downloaded from the Google Earth Engine data Catalog (https://developers.google.com/earth-engine/datasets/catalog/landsat, accessed on 27 January 2022). The Landsat satellite provides a 30 m spatial resolution of the Earth's surface about once every two weeks. A combination of the Landsat 5 Thematic Mapper (TM), Landsat 7 Enhanced Thematic Mapper (ETM), and Landsat 8 Operational Land Imager (OLI) for 2000 and 2020 was used in our study (Figure 3).
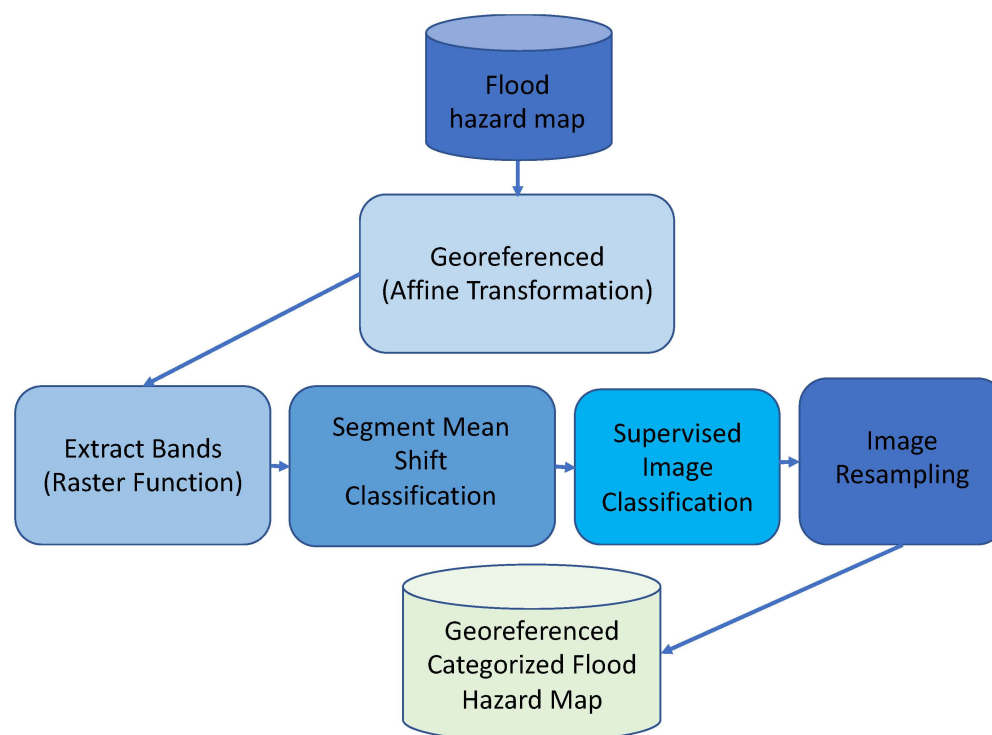
**Figure 3.** Work process for flood-hazard-category extraction.

2.1.2. World Settlement Footprint (WSF)

The WSF, which was produced by [13], represented the reference data (Figure 4a used to assess our classification accuracy. Its 10 m spatial resolution binary class, which represents the extent of human settlements globally, was used to test the accuracy of our classified product (Figure 4b). The WSF was derived by taking the means of 2014–2015 multitemporal Landsat-8 and Sentinel-1 imagery (~217,000 and ~107,000 scenes were processed, respectively).

2.1.3. Flood Inventory

In assessing the flood occurrence within the megacities, we compiled historical flood information for the twelve megacities from Dartmouth Flood Observatory (DFO, [14]), reputable online news sources, and the literature [10,15]. Flood events dating back to the 1980s were identified for some megacities such as Mexico City, Guangzhou, Lagos, and Jakarta. However, we only selected flood events that coincided with the start of our temporal analysis, which is the year 2000. From the DFO record, we found flood reports from multiple causes for some cities, but only floods from heavy rainfall were selected.
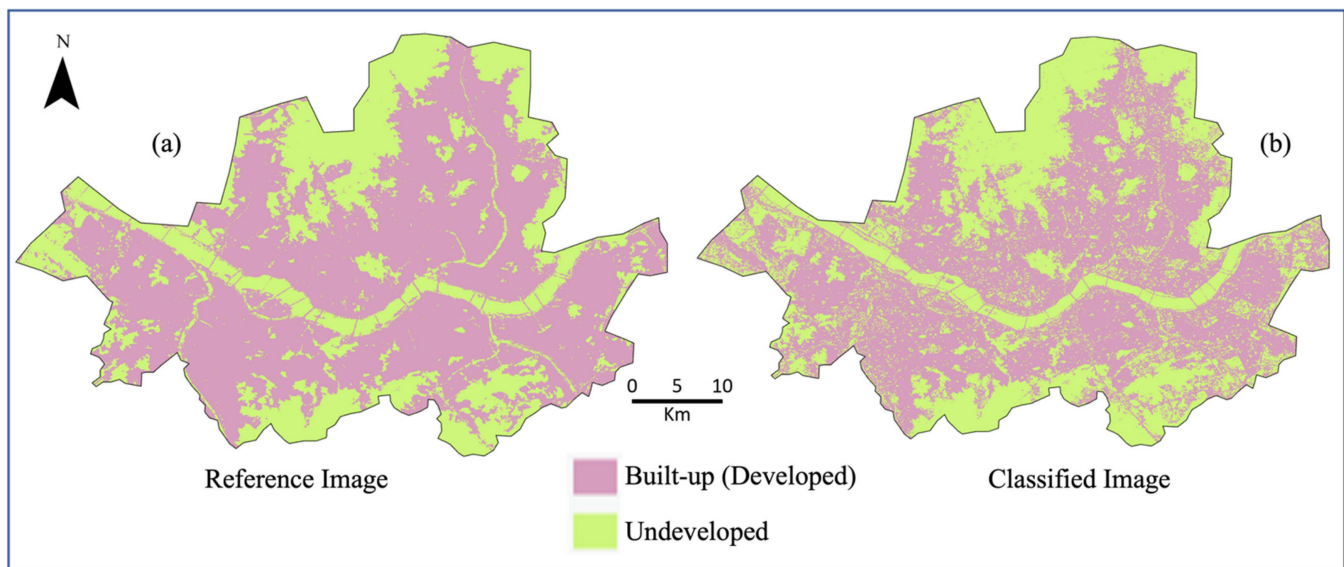
Figure 4. Sample classified images for Seoul, South Korea: (**a**) Landsat ETM 2015 classified using the unsupervised image classification method and (**b**) reference image by the World Settlement Footprint for 2015.

2.1.4. Global Facility for Disaster Reduction and Recovery (GFDRR) Flood Hazard

The GFDRR developed an analytical tool (ThinkHazard—https://thinkhazard.org/en/, accessed on 17 June 2022) for the purpose of improving knowledge and understanding of some natural hazards. It was adopted for core use in project planning by the World Bank. Specifically, the analytical tool provides hazard information about ten phenomena triggered by Earth's hydrologic, meteorological, and geophysical processes. It was developed with the intent of providing users with multi-hazard information about their project area to enable a more detailed and focused risk assessment of the hazard's influence on proposed projects. Hydraulic hazards (e.g., urban floods), the hazard of interest to this work, were characterized by the occurrence, movement, and distribution of surface and subsurface fresh and saltwater connected to the hydrologic cycle and thus affected by anthropogenic and meteoclimatic processes. Hazard levels (high, medium, low, and very low) were estimated using a probabilistic approach, which produced the frequency and severity data used in their analysis. These were estimated by three administrative units globally. The hazard data are also available as index data, showing the susceptibility of an area to a hazard.

2.2. Method

2.2.1. Image Classification and Change Detection

In order to analyze the different urban expansion patterns occurring within the megacities, the spatial distribution of the built-up lands within the cities needs to be identified through the image classification and change-detection processes. Prior to classifying the imageries, we created a composite map of our study areas using five bands representing the red, green, blue, near infrared, and shortwave infrared. We used this band combination to improve the spectral intensities of features on the maps. The Landsat images were all classified using the iso cluster unsupervised image classification method, which employs an ISODATA algorithm to automatically segregate the pixels of the images into groups of similar spectral reflectance. This image classification method uses several "clustering" statistics, where classes of pixels were created based on their shared spectral signatures. We used this method as opposed to supervised image classification because, despite using the band combination specified previously, the composite images derived for some of the study areas (e.g., Guangzhou, Cairo, and Lagos) had a low spatial and spectral resolution, which made the identification of features having similar spectral signatures challenging. The

Google Earth Engine platform was used in performing the image classification. The images were classified into 13 clusters, which were further classified into developed and undeveloped land cover. The developed and undeveloped categories were adopted from [10,15]. Change detection between images from the two time periods was performed using the compute change tool in the image analyst toolset in ArcGIS Pro 2.8.0.

2.2.2. Image Classification Validation through an Accuracy Assessment

In our image classification, built-up areas represent the developed land cover within the study areas for 2000 and 2020. To assess the accuracy of the image classification method, we compared the classified image (developed land cover) using the unsupervised image classification (Iso Cluster—Figure 4b) method to the WSF product (reference image—Figure 4a), which has a higher spatial resolution and was produced using classification schemes based on support vector machines. First, we resampled both products to the same spatial resolutions for consistency between our classified images and the reference image (WSF). Next, we applied the error matrix statistical method, which quantitatively computes and compares the accuracy of the classified image to the reference image. We created 1000 stratified random sampling points for this assessment, and two classes of land cover, which were the classes of interest, were used. They were the built-up (developed) and undeveloped (all other) landcover types. The kappa classification in Table 1 was adopted for assessing the agreement between the classified and reference images.

Table 1. Cohen Kappa Classification.

Cohen's Kappa	Interpretation
0	No agreement
0.10–0.20	Slight agreement
0.21–0.40	Fair agreement
0.41–0.60	Moderate agreement
0.61–0.80	Substantial agreement
0.81–0.99	Near perfect agreement
1	Perfect agreement

2.2.3. Urban Expansion Pattern Analysis

The megacities' three types of urban expansion patterns (edge expansion, leapfrogging, and infilling) were estimated by adopting the methods of [12,16]. We employed Equation (1), basically based on a geospatial buffer analysis showing the relationship between the old and newly developed patches (built-up land) within a defined buffer distance of 30 m—a distance corresponding to the spatial resolution of the Landsat images. In Equation (1), S, Ao, and Av were defined as the expansion pattern for a newly grown patch, the intersection between the buffer zone and the occupied category, and the intersection between the buffer zone and the vacant category. The expansion pattern is infilling when $S > 50$, edge expansion when $0 < S \leq 50$, and leapfrogging when $S = 0$.

$$S = 100 \times \left(\frac{A_0}{A_0 + A_v} \right) \tag{1}$$

The dominant urban expansion type (*DET*) was computed using Equation (2), where *APi* is the area of individual patches corresponding to an *S* value.

$$DET(s) = \sum_{i=1}^{n} AP_i \tag{2}$$

In order to assess the proportion of each urban expansion pattern (that is, the quantity of developed land between 2000 and 2020) within each megacity, Equation (3) was adopted,

where *P* is the percentage of an urban expansion pattern and *At* is the total area of built-up land for 2020.

$$P = \frac{DET(s)}{A_t} \times 100 \qquad (3)$$

2.2.4. Flood-Hazard Classification

To estimate the association of the three urban expansion patterns to flooding, we utilized the probabilistic data presented by ThinkHazard version 2, which can be assessed in their GitHub repository (https://github.com/GFDRR/thinkhazard, accessed on 17 June 2022) and as maps of categorized flood-hazard levels (urban, river, and coastal) globally. The unreferenced flood-hazard maps for the twelve megacities were acquired, georeferenced, and classified using the workflow in Figure 3.

As a simple qualitative validation of the ThinkHazard (TH) flood-hazard map using the Dartmouth Flood Observatory (DFO) flood reports, we applied a GIS query to compare areas where the DFO reported floods to the areas which the TH delineated as having medium to high flood-hazard levels. Furthermore, we compiled the general flood-hazard levels for the twelve megacities delineated by TH (Table 2).

Table 2. ThinkHazard flood-hazard levels for the megacities.

Megacities	Countries	Urban Flood	River Flood	Coastal Flood
Guangzhou	China	High	High	High
Tokyo	Japan	High	High	High
Jakarta	Indonesia	High	High	High
Seoul	South Korea	Medium	Low	No Data
Mexico City	Mexico	High	High	No Data
São Paulo	Brazil	Low	Medium	No Data
Cairo	Egypt	High	High	No Data
Lagos	Nigeria	High	High	Medium
Los Angeles	USA	Very Low	Very Low	High
Moscow	Russia	Low	High	No Data
Buenos Aires	Argentina	High	High	High
London	Great Britain	Low	Medium	High

2.2.5. Statistical Test of the Metrics of Urban Expansion Patterns and the ThinkHazard Flood-Hazard Zone

One of the objectives of this work is to gain insight into the association of the three urban expansion patterns with flood conditions. In this scenario, for the ThinkHazard flood-hazard zones, we applied Pearson's Correlation Coefficient to measure the relationship between the quantity of occurrence of each of the three urban expansion patterns within the flood-hazard zones. The significance of this relationship was quantified first by specifying a null hypothesis that there is no significant correlation between the quantity of each urban expansion pattern within the flood-hazard zone. The alternative hypothesis is that there is a significant correlation between the quantity of each urban expansion pattern within the ThinkHazard flood-hazard zone. Next, using the *t*-test inferential statistics, we computed the *p*-value after setting our significance level to 0.05.

3. Results

3.1. Image Classification Accuracy Assessment

To ascertain the accuracy of our image classification, we computed a confusion matrix. Table 3 shows the result of the assessment between the reference (Figure 4a) and classified image (Figure 4b). Overall, the kappa coefficient was 0.67, which explains the substantial agreement (Table 3) between the built-up areas identified by our image classification method and the World Settlement Footprint method.

Table 3. Error Matrix Computation Summary.

Land Cover Class		Reference Image (World Settlement Footprint (WSF))				
		Built-Up (Developed)	Undeveloped	Total	User's Accuracy	Kappa
Classified Image	Built-up (Developed)	554	45	599	0.92	0
	Undeveloped	111	290	401	0.72	0
Total		665	335	1000	0	0
Producer's Accuracy		0.83	0.87	0	0.84	0
Kappa		0	0	0	0	0.67

3.2. Spatiotemporal Urban Developments of the Megacities

Table 4 illustrates an estimated quantity of built-up land in 2000 and 2020 in the megacities. Among the twelve cities, we found Guangzhou in China to have the highest area, estimated to be 7100 km^2, followed by Lagos in Nigeria and Cairo in Egypt, with an estimated area of 3726 km^2 and 3085 km^2, respectively. Guangzhou's built-up area in 2000 was 1652 km^2; by 2020, it had grown by an additional 2166 km^2. Lagos, in 2000 had a built-up area of 596 km^2 which experienced a growth of 1113 km^2 in the built-up area by 2020. The growth rates in the development of Guangzhou and Lagos were estimated to be 76% and 54%, respectively. The percentages of urban growth experienced by the megacities with respect to their total were calculated and shown in Table 4. In 2000, some cities such as Guangzhou, Cairo, and Lagos had percentages of built areas within a range of 16% and 25%, making them the cities with the least built-up area. However, by 2020, compared to the rest, some megacities had relatively substantial growth in built-up land by 2000, up to an additional ~30% of their total area; examples are Guangzhou and Lagos.

Table 4. Megacities' Built-up Land Percentages.

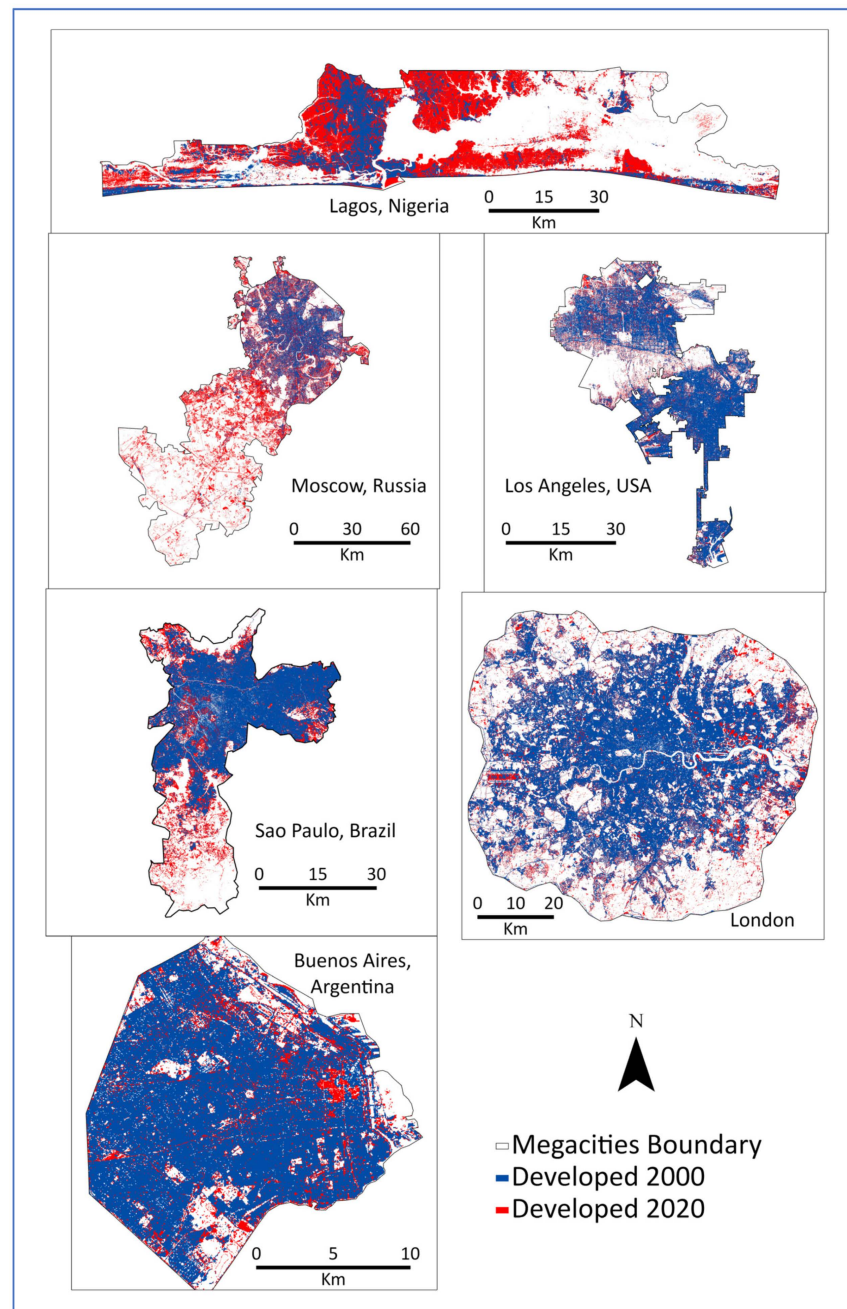| Megacities	Built-Up Area 2000 (km^2)	Built-Up Area 2020 (km^2)	Total Area (km^2)	Percentage (%) Built-Up 2000	Percentage (%) Built-Up 2020	Percentage (%) Built-Up Land
Guangzhou	1652	2166	7100	23.27	30.51	53.77
Tokyo	999	305	1823	54.80	16.73	71.53
Jakarta	417	84	664	62.80	12.65	75.45
Seoul	387	92	605	63.97	15.21	79.17
Mexico City	588	264	1484	39.62	17.79	57.41
Cairo	524	354	3085	16.99	11.47	28.46
Lagos	596	1113	3726	16.00	29.87	45.87
Buenos Aires	177	31	209	84.69	14.83	99.52
Los Angeles	757	162	1239	61.10	13.08	74.17
Moscow	735	953	2510	29.28	37.97	67.25
London	1532	373	2321	66.01	16.07	82.08
São Paulo	797	272	1523	52.33	17.86	70.19

Conversely, cities with more than 50% built-up area in 2000 experienced between ~12% and 18% urban growth in 2020. We found the magnitude of the percentage of built-up area (urban development) for the megacities to exhibit a pattern with the cities' total area or extent. This relationship, as assessed using Pearson's Correlation Coefficient, was −0.61.

Figures 5 and 6 present the visualization of the change dynamics of development in the cities for the years 2000 and 2020. For example, for Guangzhou (Figure 5) and Lagos (Figure 6), the substantial amount of developed land between 2000 (blue) and 2020 (red) could be perceived, which could imply rapid urbanization in the cities.
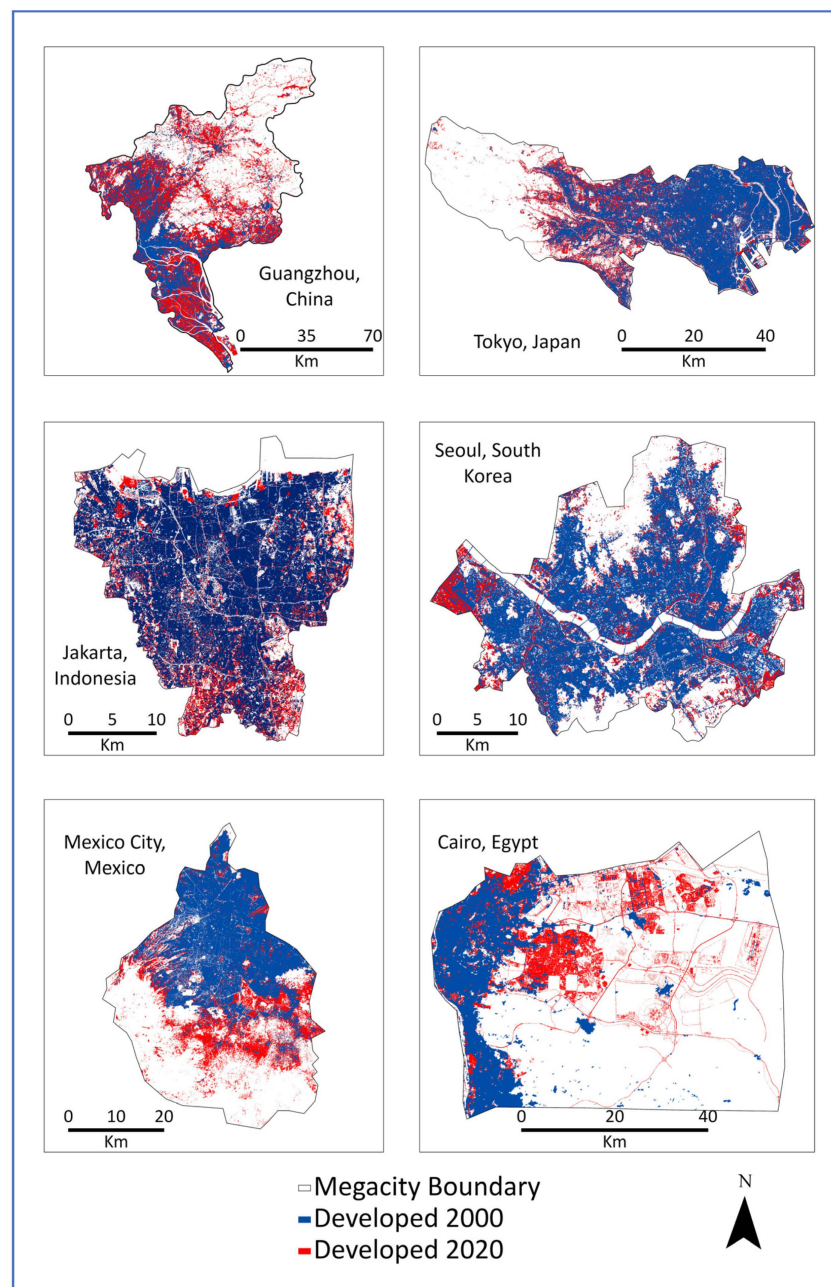
Figure 5. Spatiotemporal Distribution of Built-up Areas in Guangzhou, Tokyo, Jakarta, Seoul, Mexico City, and Cairo for the years 2000 and 2020.

Figure 6. Spatiotemporal Distribution of Built-up Areas in Moscow, Los Angeles, Sao Paulo, London, and Buenos Aires for the years 2000 and 2020.
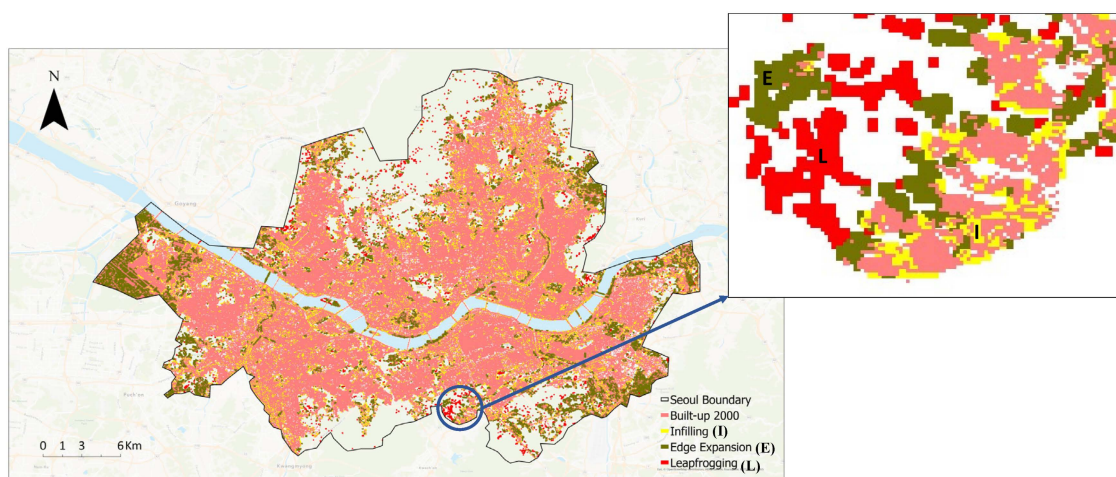
3.3. Urban Expansion Pattern

Using Equation (1), we computed the S values for the twelve megacities. The most dominant expansion pattern within the cities was also computed using Equation (2). Table 5 shows that the dominant expansion pattern in eight cities (Guangzhou, Tokyo, Jakarta, Seoul, Mexico City, Sao Paulo, Lagos, and Moscow) is edge expansion, while the pattern in four cities (Cairo, Los Angeles, Buenos Aires, and London) is infilling.

Table 5. Megacities and associated dominant urban expansion patterns based on patch size and number.

| ID	Megacity	Dominant Urban Expansion Type Based on Patch Size (Area) (2000–2020)	Dominant Urban Expansion Type Based on the Number of Patches (Area) (2000–2020)
1	Guangzhou	Edge Expansion	Infilling
2	Tokyo	Edge Expansion	Infilling
3	Jakarta	Edge Expansion	Infilling
4	Seoul	Edge Expansion	Infilling
5	Ciudad de Mexico	Edge Expansion	Infilling
6	Sao Paulo	Edge Expansion	Infilling
7	Cairo	Infilling	Leapfrogging
8	Lagos	Edge Expansion	Infilling
9	Los Angeles	Infilling	Infilling
10	Moscow	Edge Expansion	Infilling
11	Buenos Aires	Infilling	Infilling
12	London	Infilling	Infilling

Figure 7 is a pictorial representation of an example of infilling, edge expansion, and leapfrogging urban expansion patterns in Seoul, South Korea (and, by extension, the megacities), which provides perspective on how the patterns of developments are spatially distributed. The red, yellow, and green pixels represent leapfrogging, infilling, and edge expansion, respectively.

Figure 7. Visual example of infilling, edge expansion, and leapfrogging urban expansion pattern in Seoul, South Korea, between 2000 and 2020.

We found a robust negative correlation with statistical significance < 0.05 between the areas of the expansion patterns and the number of patches of developed land (Figure 8) for all the megacities. The percentage of their areas with respect to the total developed area between 2000 and 2020 is shown in Figure 9. From Figure 9, the city of Guangzhou and Lagos seems to display a similar percentage of the three expansion patterns. Generally, we identified some similar percentages among the megacities, as shown in Figure 9. Other examples are Tokyo and Jakarta; Buenos Aires and Los Angeles; London and Cairo; and Sao Paulo, Mexico City, and Moscow.
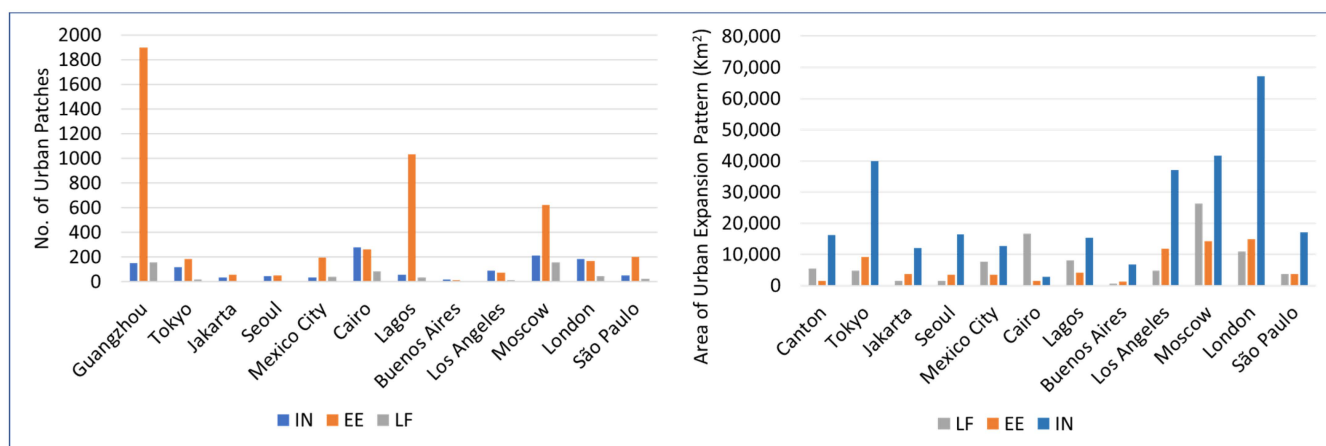
Figure 8. Graphical representation of the areas and the number of patches for infilling, edge expansion, and leapfrogging for the megacities between 2000 and 2020.
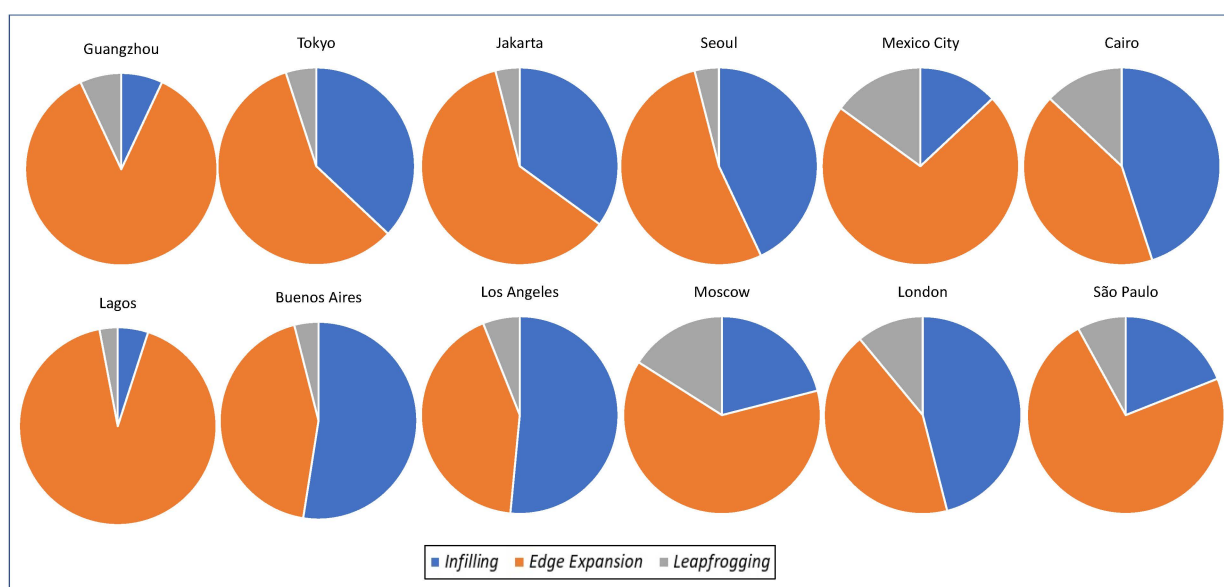
Figure 9. Percentage of infilling, edge expansion, and leapfrogging urban expansion patterns in the megacities between 2000 and 2020.

3.4. Heavy Rainfall Triggered Floods in Megacities

From the Dartmouth Flood Observatory flood report, several sources of flooding were cited for some of the cities, but the prevalent source of flooding common to all the cities was heavy rainfall. Our compilation of the flood inventory, including flood source, year(s), and flood occurrence, shows heavy rainfall to be the most cited cause of flooding in these cities. We also found that all these cities have all experienced devastating floods at least twice, with Jakarta, Seoul, Sao Paulo, Lagos, and London having a flood event that occurred during the compilation of this work (2022) and Los Angeles in 2023 (Table 6).

Table 6. Flood inventory for the twelve megacities and flood sources [10,14,15].

| Megacity	Country	Population	Climate	Flood (Yes/No)	Year	Flood_Source
Guăngzhōu	China	15,300,000	Humid subtropical to tropical climate	Yes	2000, 2001, 2004, 2005, 2007, 2010, 2020.	Heavy Rainfall
Tōkyō	Japan	31,900,000	Humid subtropical	Yes	2000, 2008, 2019.	Heavy Rainfall
Jakarta	Indonesia	26,500,000	Tropical humid	Yes	2001–2004, 2006–2010, 2012–2014, 2016, 2020–2022.	Heavy Rainfall
Seoul	Korea (South)	20,700,000	Temperate	Yes	2001, 2003, 2004, 2006, 2010, 2011, 2022.	Heavy Rainfall
Ciudad de México	Mexico	21,505,000	Subtropical	Yes	2008, 2009, 2010, 2011, 2021.	Heavy Rainfall
São Paulo	Brazil	22,495,000	Temperate	Yes	2000, 2001, 2003–2005, 2007–2011, 2014, 2016, 2018, 2019, 2022.	Heavy Rainfall
Al-Qāhirah	Egypt	19,787,000	Subtropical desert	Yes	2010, 2011, 2018–2021.	Heavy Rainfall
Lagos	Nigeria	15,487,000	Tropical	Yes	2000, 2002, 2004, 2007, 2012, 2018–2022.	Heavy Rainfall
Los Angeles	United States of America	15,477,000	Subtropical	Yes	2003, 2005, 2010, 2017, 2018, 2023.	Heavy Rainfall
Moskva	Russia	17,693,000	Continental	Yes	2004, 2020, 2021.	Heavy Rainfall
Buenos Aires	Argentina	16,216,000	Temperate	Yes	2001, 2013, 2016, 2017.	Heavy Rainfall
London	Great Britain	11,120,000	Temperate	Yes	2000, 2003, 2008, 2009,2012, 2014, 2020–2022.	Heavy Rainfall

3.5. Urban Expansion Pattern and ThinkHazrd Flood-Hazard Zones

In our comparison of the Dartmouth Flood Observatory (DFO) to the ThinkHazard (TH) flood-hazard classes, we found that cities such as Sao Paulo, Los Angeles, Moscow, and London, were classified as having a low to very low urban flood hazard. These cities were reported to have experienced recent floods (Table 6) in the DFO flood report. The discrepancy in the DFO and TH datasets is because the DFO does not include the types of floods but the sources of floods and actual occurrences. As a result, our analysis of the association of the three urban expansion patterns with flooding was performed in Guangzhou, Tokyo, Jakarta, Seoul, Mexico City, Cairo, Lagos, and Buenos Aires, where the DFO reported flood and the TH flood hazard is medium to high urban flood. In these eight cities, the DFO and TH flood-hazard maps demonstrated some agreement. Figure 10 displays the spatial distribution of the three types of expansion patterns in Jakarta and Mexico City within the areas classified as depicting a medium to high flood hazard. Generally, the edge expansion urban expansion pattern seems to be predominantly associated with the flood-hazard zones in Buenos Aires, Lagos, Mexico City, Seoul, Jakarta, Tokyo, and Guangzhou, while the infilling pattern was dominant in Cairo (Figure 11). Though the area of the infilling pattern in the flood-hazard zone dominant in Cairo, we found that its total area was 19.5 km^2 while the edge expansion was 17.3 km^2. In the eight cities, the area of the infilling expansion pattern associated with the flood-hazard zone was relatively high in all the cities. Meanwhile, the area of the leapfrogging pattern, on the other hand, displayed some association with flood hazard, though not as much as the edge expansion but more than the infilling expansion pattern in Guangzhou and Mexico City.
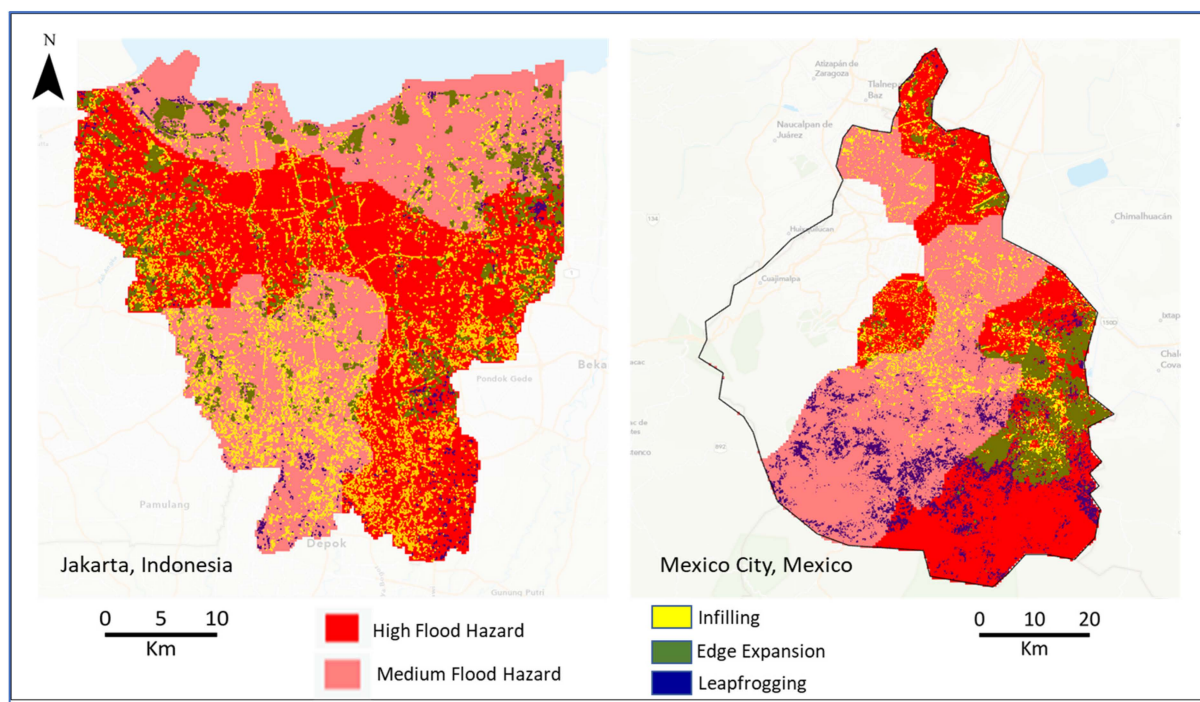
Figure 10. Example of urban expansion patterns for Jakarta and Mexico City overlay on the TH flood-hazard map.
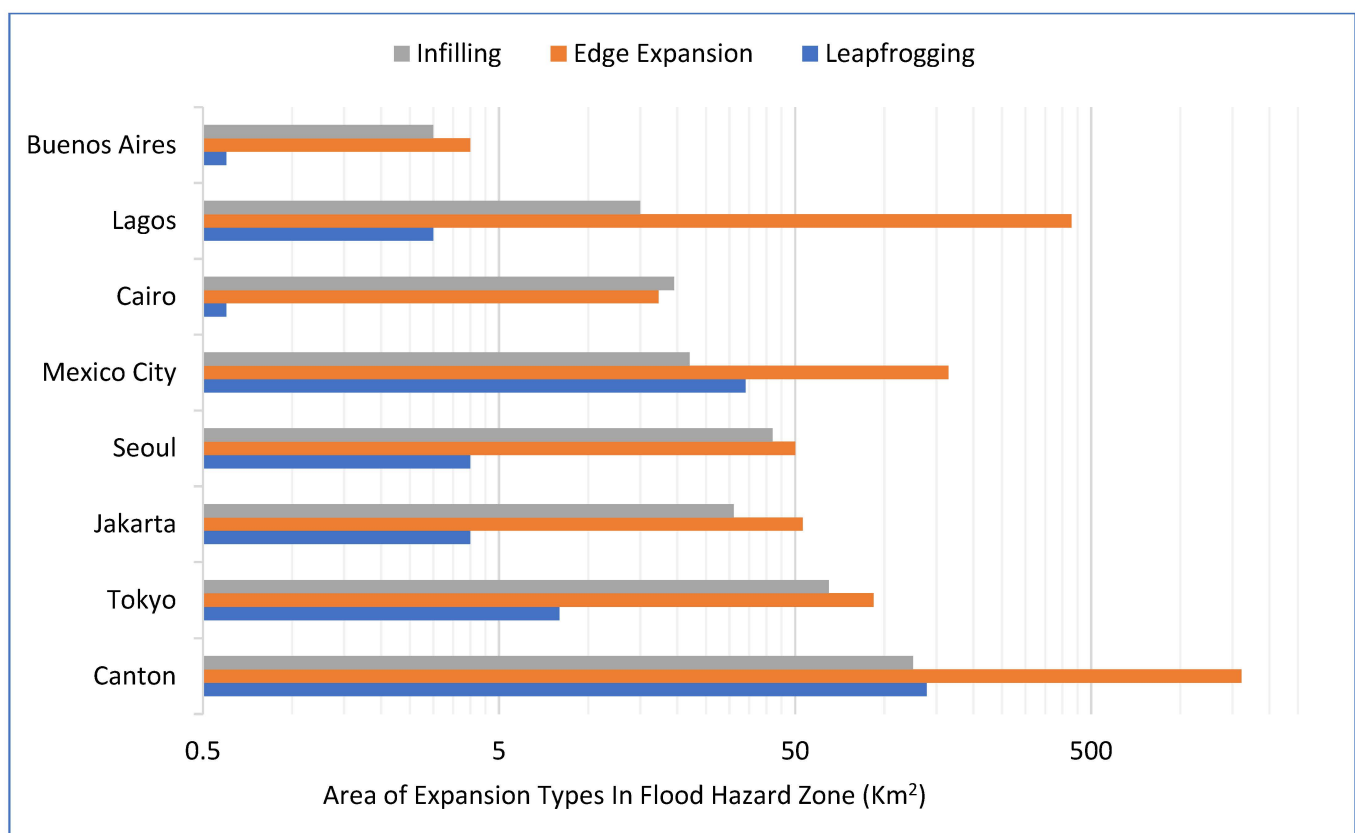
Figure 11. Areas of infilling, edge expansion, and leapfrogging urban expansion pattern for the megacities on a logarithmic scale.

3.6. Statistical Significance of Urban Expansion Pattern Association with Flood Hazard

From our statistical comparison of the areas of the three urban expansion patterns associated with the ThinkHazard flood-hazard zones in the megacities tested, Table 7 shows that we can reject the null hypothesis that there is no significant correlation between the quantity of each urban expansion pattern within the ThinkHazard flood-hazard zone. Additionally, our statistical test showed that the edge expansion and leapfrogging pattern displayed a very strong positive correlation coefficient of 0.96 and 0.85, respectively, while the infilling pattern showed a weak positive correlation of 0.3. The significance of these correlations displayed in Table 7 shows that the edge expansion and leapfrogging patterns have a *p*-value lower than 0.05, while the infilling pattern has a *p*-value greater than 0.05.

Table 7. Inferential Summary Statistics for the Spatial Distribution of Urban Expansion Patterns within the ThinkHazard Flood-hazard Zone. *p*-Value Threshold = 0.05.

	Correlation Coefficient (r)	*p*-Value
Leapfrogging	0.85	0.08
Edge Expansion	0.96	0.0002
Infilling	0.3	0.5

4. Discussion

4.1. Flooding in Megacities

Our rationale in assessing flood occurrence in megacities stemmed from our assumption that urbanization is fueled by increased population and economic development, and as such, global cities of the world with a population of over 10 million inhabitants [17,18] would be at risk of environmental hazards such as flooding [19]. Consequently, these cities would serve as study sites for exploring the different patterns of urban expansion associated with flooding. Based on these assumptions, our compilation of flood inventory from the DFO, online, and the literature revealed flooding in all the twelve megacities resulting from heavy rainfall. Recurring flooding in these megacities, as documented by various sources [10,14,20,21], could not have occurred randomly but rather buttresses the arguments and accounts of various researchers on the effects of urbanization in the form of urban sprawl accompanied by rapid population increase on flood risk [7,22–27]. Specifically, a coalescence of diverse drivers such as human–environmental interactions, urbanization-hydrology alteration [28,29], and natural conditions such as the physical location of these cities further exacerbates flood risk for megacities [30,31]. For example, Jakarta, Lagos, Guangzhou, Tokyo, London, Los Angeles, and Buenos Aires are all coastal cities in low-lying areas with high rates of urbanization. Naturally, the physical location of these cities makes them vulnerable to flooding and unplanned urban development activities, giving rise to more socioeconomic activities and infrastructural developments and heightening the risk. With emerging changes in climate change and intensifying precipitation, these cities should be major targets for flood resilience measures in other to foster urban sustainability.

4.2. Implications of Urban Expansion Patterns for Floods in Megacities

Our analysis of the area in square kilometers of the different urban expansion patterns for all the megacities indicated the edge expansion pattern to be the most common to all the cities, followed by the infilling pattern, and leapfrogging is the least. Analysis of the spatial association of these expansion patterns in the flood-hazard zone shows the edge expansion and leapfrogging pattern to have a significant association with the flood hazard. In contrast, the infilling pattern, though having a weak positive correlation with flood hazard, does not depict a significant association with it. The area of the edge expansion pattern within the total area of development from 2000 to 2020 for the megacities was consistently high for eight out of twelve cities, while the area of the infilling pattern was high for four cities. Meanwhile, the area of the leapfrogging pattern was consistently low in

all the megacities. These spatial variations of the areas of the three patterns are indications of their inherent characteristics. For example, the leapfrogging pattern exhibits a scattered spatial distribution characterized by small patches of land compared to edge expansion and infilling patterns [12], which reveal more compact characteristics with large patch areas. The infilling pattern, though having more areas within the flood-hazard zone, showed a weak positive correlation with flood hazard and was statistically insignificant, which could be interpreted to imply its unapparent effects over short periods [11,12].

Previous studies [11,12] that assessed the effects of edge expansion, infilling, and leapfrogging on flood risk focused more on the vulnerability element of flood risk. However, the result of our analysis also presented some potential insight into the hazard and exposure element of flood risk. Our study showed that the edge expansion and the leapfrogging pattern are significantly associated with flood hazards in megacities. This could be further interpreted to extend to the elements of flood vulnerability and exposure. Considering the relationship between the old patch and the new patch within the buffer zone, the characteristics of the infilling expansion pattern is to develop within existing patches while the edge expansion develops around the fringes of existing patches; together these patterns create a compact appearance of a tightly knitted impervious surface and hence affect hydrologic processes (rain runoff) operating within the cities [12,32]. The large area exhibited by the edge expansion patterns within the megacities could imply more exposure of urban land to flood risk, while on the other hand, the small area exhibited by the leapfrogging pattern within the megacities could imply increasing vulnerability to flooding risk due to the assumption that small locales possess few resources for flood control measures [11,12]. With the characteristics of the three expansion patterns and their influences on flooding, the situation is more heightened for developing countries with their high population densities, limited resources, urban sprawl, a lack of flood management, and urban planning policies [33].

4.3. Implication for Urban Resilience

From our findings, the edge expansion and infilling pattern were found to be dominant in the megacities, which agrees with the findings from previous urban studies in China and Brazil [11,12,34–37]. The dominance of these two patterns in the megacities provides insight into the urban landform, which is compact [35]. It has been debated that in order to achieve sustainable urban development in major cities, urban planning policies need to encourage edge expansion and infilling patterns because of their compact characteristics, which could decrease flood vulnerability by taking advantage of existing flood protection [11]. This is logical when concerns are focused on the vulnerability element of flood risk, which relates to flood-prevention measures [38]. However, from the socio-hydrology perspective [12,28], the compact nature of these urban expansion patterns could be disadvantageous because they lead to more imperviousness. When certain thresholds are exceeded, it could exacerbate flood hazards by altering infiltration and increasing surface runoff [39,40]. This could be attributed to megacities' proneness to flooding.

Additionally, for planned cities such as those in developed countries, existing flood control measures and natural and engineered drainage systems could have been designed based on past climatic regimes and lost their designed capabilities in the presence of climatic conditions which have arisen due to climate change. Improving urban resilience to flooding for these cities would involve upgrading flood management plans, which is already being implemented in the United States [41]. Developing countries are mostly lagging in terms of flood management and would require more adaptation effort to increase flood resilience.

4.4. Comparison with Previous Studies

Our research attempted to correlate patterns of urban expansion in megacities to urban flood hazard and highlight its implications for creating a holistic flood risk framework that would cater to current climate scenarios and thus provide insight into building a resilient society. Previous studies have addressed urban expansion patterns and flood occurrence from

the perspective of historical flood reports in the Yangtze River Economic Belt and North China Plain Area [11,12] and others from the standpoint of megacities and rapidly developing cities' predisposition to flooding vulnerability [42,43] and exposure [44–46]. To the knowledge of the authors, this work would be the first to highlight and present the relationship between urban expansion patterns and urban flood hazards in global megacities.

4.5. Research Limitations and Future Directions

Some limitations of this study encourage further exploration of the influence of the three urban expansion patterns on flood risk. Our study presented evidence that urban expansion patterns and their spatial distribution could influence flood exposure, vulnerability, and hazard and ultimately increase flood risk using third-party and freely available datasets (e.g., ThinkHazard flood-hazard map). This information would sensitize flood managers and urban planners to the influence of urban expansion patterns on flood risk and why flood risk frameworks or models should be interdisciplinary. Exploring this would require a more localized flood modeling using site-specific parameters to quantitatively assess the extent of flood risk in these cities. As regards the infilling pattern impact threshold, future research directions could focus on quantitatively investigating the threshold at which the infilling pattern would significantly influence flood hazard. Though its contribution to exposure was inferred, more studies could be undertaken to ascertain its impact on flood risk.

5. Conclusions

This study investigated urban growth in twelve megacities, the pattern of growth, the dominant and common growth pattern, and how this pattern could be contributing to flooding in these cities. Our focus was to find the link between the urban expansion patterns (infilling, edge expansion, and leapfrogging) and flooding in urbanized cities, and appropriate examples were cities with the highest possible population, and hence urbanization. We examined the flood history of these cities, and our findings showed that all the megacities had experienced devastating flooding in the recent past and during the analysis of this work, citing heavy rainfall as the source. Furthermore, we explored the land changes in these cities between 2000 and 2020 and investigated the patterns of change experienced by these cities. Our analysis showed that some of the megacities have developed more than 60% of their entire land area, while cities such as Guangzhou and Lagos, while having the highest land area, have developed more than 40% of their entire land area, thereby suggesting rapid urbanization. This study also found these megacities exhibit edge expansion and infilling urban expansion patterns. Eight out of twelve megacities exhibit the edge expansion pattern, making it the most common in all the cities. Exploring the association of the spatial distribution of the areas (km^2) of the patterns of expansion within the flood-hazard zone using the ThinkHazard flood-hazard map showed the edge expansion pattern to have more spatial distribution within the flood-hazard zone, followed by infilling and leapfrogging. Though the three patterns were associated with flooding at varying spatial distributions within the flood-hazard zone, we found that the edge expansion and leapfrogging pattern had more statistical significance, while the infilling did not. Generally, our work presents a synopsis of flooding due to heavy rainfall in megacities and how the three patterns of urban growth in highly populated and urbanized cities could contribute to their flood disposition. This information is crucial to building flood resilience for these cities, especially with climate change intensifying rainfall. It also suggests that future urban planning should integrate flood management plans.

Author Contributions: Conceptualization, D.I. and W.Z.; methodology, D.I. and W.Z.; software, D.I.; validation, D.I.; formal analysis, D.I.; investigation, D.I.; resources, D.I.; writing—D.I.; writing—review and editing, D.I. and W.Z.; visualization, D.I. All authors have read and agreed to the published version of the manuscript.

Abbreviations

BLF	Built-up Land in Floodplain
DFO	Dartmouth Flood Observatory
ETM	Enhanced Thematic Mapper
GFDRR	Global Facility for Disaster Reduction and Recovery
LULC	Land Use and Land Cover
OLI	Operational Land Imager
TH	ThinkHazard
TM	Thematic Mapper
WSF	World Settlement Footprint

References

1. Rentschler, J.; Salhab, M.; Jafino, B.A. Flood exposure and poverty in 188 countries. *Nat. Commun.* **2022**, *13*, 3527. [CrossRef] [PubMed]
2. Brøgger, D. Urban diaspora space: Rural–urban migration and the production of unequal urban spaces. *Geoforum* **2019**, *102*, 97–105. [CrossRef]
3. Delgado Wise, R.; Márquez Covarrubias, H.; Puentes, R. Reframing the debate on migration, development and human rights. *Popul. Space Place* **2013**, *19*, 430–443. [CrossRef]
4. United Nations. *World Population Prospects. The 2004 Revision*; Volume III: Analytical Report; United Nations: New York, NY, USA, 2006.
5. Konrad, C.P. *Effects of Urban Development on Floods*; Christopher P. Konrad: Tacoma, WA, USA, 2003.
6. Hollis, G.E. The effect of urbanization on floods of different recurrence interval. *Water Resour. Res.* **1975**, *11*, 431–435. [CrossRef]
7. Sheng, J.; Wilson, J.P. Watershed urbanization and changing flood behavior across the Los Angeles metropolitan region. *Nat. Hazards* **2009**, *48*, 41–57. [CrossRef]
8. Skougaard Kaspersen, P.; Høegh Ravn, N.; Arnbjerg-Nielsen, K.; Madsen, H.; Drews, M. Comparison of the impacts of urban development and climate change on exposing European cities to pluvial flooding. *Hydrol. Earth Syst. Sci.* **2017**, *21*, 4131–4147. [CrossRef]
9. Rosenzweig, C.; Solecki, W.D.; Romero-Lankao, P.; Mehrotra, S.; Dhakal, S.; Ibrahim, S.A. (Eds.) *Climate Change and Cities: Second Assessment Report of the Urban Climate Change Research Network*; Cambridge University Press: New York, NY, USA, 2018.
10. Idowu, D.; Zhou, W. Land Use and Land Cover Change Assessment in the Context of Flood Hazard in Lagos State, Nigeria. *Water* **2021**, *13*, 1105. [CrossRef]
11. Han, Y.; Huang, Q.; He, C.; Fang, Y.; Wen, J.; Gao, J.; Du, S. The growth mode of built-up land in floodplains and its impacts on flood vulnerability. *Sci. Total Environ.* **2020**, *700*, 134462. [CrossRef]
12. Wang, G.; Hu, Z.; Liu, Y.; Zhang, G.; Liu, J.; Lyu, Y.; Gu, Y.; Huang, X.; Zhang, Q.; Tong, Z.; et al. Impact of expansion pattern of built-up land in floodplains on flood vulnerability: A case study in the North China Plain area. *Remote Sens.* **2020**, *12*, 3172. [CrossRef]
13. Marconcini, M.; Metz-Marconcini, A.; Üreyen, S.; Palacios-Lopez, D.; Hanke, W.; Bachofer, F.; Zeidler, J.; Esch, T.; Gorelick, N.; Kakarla, A.; et al. Outlining where humans live, the World Settlement Footprint 2015. *Sci. Data* **2020**, *7*, 242. [CrossRef]
14. Brakenridge, G.R. *Global Active Archive of Large Flood Events*; Dartmouth Flood Observatory, University of Colorado: Boulder, CO, USA, 2010.
15. Idowu, D. Assessing the Utilization of Remote Sensing and GIS Techniques for Flood Studies and Land Use/Land Cover Analysis Through Case Studies in Nigeria and the USA. Ph.D. Thesis, Colorado School of Mines, Golden, CO, USA, 2021.
16. Liu, X.; Li, X.; Chen, Y.; Tan, Z.; Li, S.; Ai, B. A new landscape index for quantifying urban expansion using multi-temporal remotely sensed data. *Landsc. Ecol.* **2010**, *25*, 671–682. [CrossRef]
17. Bocquier, P. World Urbanization Prospects: An alternative to the UN model of projection compatible with the mobility transition theory. *Demogr. Res.* **2005**, *12*, 197–236. [CrossRef]
18. Kraas, F. Megacities and global change: Key priorities. *Geogr. J.* **2007**, *173*, 79–82. [CrossRef]
19. Kraas, F. Megacities as global risk areas. In *Urban Ecology*; Springer: Boston, MA, USA, 2008; pp. 583–596.
20. Nkwunonwo, U.C.; Whitworth, M.; Baily, B. A review and critical analysis of the efforts towards urban flood risk management in the Lagos region of Nigeria. *Nat. Hazards Earth Syst. Sci.* **2016**, *16*, 349–369. [CrossRef]
21. Idowu, D.; Zhou, W. Performance evaluation of a potential component of an early flood warning system—A case study of the 2012 flood, Lower Niger River Basin, Nigeria. *Remote Sens.* **2019**, *11*, 1970. [CrossRef]

22. Ajjur, S.B.; Al-Ghamdi, S.G. Exploring urban growth–climate change–flood risk nexus in fast growing cities. *Sci. Rep.* **2022**, *12*, 12265. [CrossRef]

23. Li, G.F.; Xiang, X.Y.; Tong, Y.Y.; Wang, H.M. Impact assessment of urbanization on flood risk in the Yangtze River Delta. *Stoch. Environ. Res. Risk Assess.* **2013**, *27*, 1683–1693. [CrossRef]

24. Chen, Y.; Zhou, H.; Zhang, H.; Du, G.; Zhou, J. Urban flood risk warning under rapid urbanization. *Environ. Res.* **2015**, *139*, 3–10. [CrossRef]

25. Bahrawi, J.; Ewea, H.; Kamis, A.; Elhag, M. Potential flood risk due to urbanization expansion in arid environments, Saudi Arabia. *Nat. Hazards* **2020**, *104*, 795–809. [CrossRef]

26. Abdelkarim, A.; Gaber, A.F.; Alkadi, I.I.; Alogayell, H.M. Integrating remote sensing and hydrologic modeling to assess the impact of land-use changes on the increase of flood risk: A case study of the Riyadh–Dammam train track, Saudi Arabia. *Sustainability* **2019**, *11*, 6003. [CrossRef]

27. Saghir, J.; Santoro, J. Urbanization in Sub-Saharan Africa. In *Meeting Challenges by Bridging Stakeholders*; Center for Strategic & International Studies: Washington, DC, USA, 2018.

28. Sivapalan, M.; Savenije, H.H.; Blöschl, G. Socio-hydrology: A new science of people and water. *Hydrol. Process.* **2012**, *26*, 1270–1276. [CrossRef]

29. Environmental Protection Agency. *Urbanization and Population Change*; Report on the Environment. (Retrieved 08/21/2022); Environmental Protection Agency: Washington, DC, USA, 2022.

30. Dewan, A.M. Hazards, risk, and vulnerability. In *Floods in a Megacity*; Springer: Dordrecht, The Netherlands, 2013; pp. 35–74.

31. Dewan, A. *Floods in a Megacity: Geospatial Techniques in Assessing Hazards, Risk and Vulnerability*; Springer: Dordrecht, The Netherlands, 2013; pp. 119–156.

32. De Mello Silva, C.; da Silva, G.B.L. Cumulative effect of the disconnection of impervious areas within residential lots on runoff generation and temporal patterns in a small urban area. *J. Environ. Manag.* **2020**, *253*, 109719. [CrossRef]

33. Montoya, L. Geo-data acquisition through mobile GIS and digital video: An urban disaster management perspective. *Environ. Model. Softw.* **2003**, *18*, 869–876. [CrossRef]

34. Huang, X.; Xia, J.; Xiao, R.; He, T. Urban expansion patterns of 291 Chinese cities, 1990–2015. *Int. J. Digit. Earth* **2019**, *12*, 62–77. [CrossRef]

35. Li, Z.; Gurgel, H.; Li, M.; Dessay, N.; Gong, P. Urban land expansion from scratch to urban agglomeration in the Federal District of Brazil in the past 60 years. *Int. J. Environ. Res. Public Health* **2022**, *19*, 1032. [CrossRef]

36. Hao, R.; Su, W.; Yu, D. Quantifying the type of urban sprawl and dynamic changes in Shenzhen. In *International Conference on Computer and Computing Technologies in Agriculture*; Springer: Berlin/Heidelberg, Germany, 2012; pp. 407–415.

37. Fang, C.; Zhao, S. A Comparative study of spatiotemporal patterns of urban expansion in six major cities of the Yangtze River Delta from 1980 to 2015. *Ecosyst. Health Sustain.* **2018**, *4*, 95–114. [CrossRef]

38. Bae, S.; Chang, H. Urbanization and floods in the Seoul Metropolitan area of South Korea: What old maps tell us. *Int. J. Disaster Risk Reduct.* **2019**, *37*, 101186. [CrossRef]

39. Sohn, W.; Kim, J.H.; Li, M.H.; Brown, R.D.; Jaber, F.H. How does increasing impervious surfaces affect urban flooding in response to climate variability? *Ecol. Indic.* **2020**, *118*, 106774. [CrossRef]

40. Du, S.; Shi, P.; Van Rompaey, A.; Wen, J. Quantifying the impact of impervious surface location on flood peak discharge in urban areas. *Nat. Hazards* **2015**, *76*, 1457–1471. [CrossRef]

41. Jongman, B. Effective adaptation to rising flood risk. *Nat. Commun.* **2018**, *9*, 1986. [CrossRef]

42. Mitchell, J.K. Megacities and natural disasters: A comparative analysis. *GeoJournal* **1999**, *49*, 137–142. [CrossRef]

43. Hunt, J.C.; Aktas, Y.D.; Mahalov, A.; Moustaoui, M.; Salamanca, F.; Georgescu, M. Climate change and growing megacities: Hazards and vulnerability. *Proc. Inst. Civ. Eng.-Eng. Sustain.* **2017**, *171*, 314–326. [CrossRef]

44. Li, C.; Liu, M.; Hu, Y.; Wang, H.; Zhou, R.; Wu, W.; Wang, Y. Spatial distribution patterns and potential exposure risks of urban floods in Chinese megacities. *J. Hydrol.* **2022**, *610*, 127838. [CrossRef]

45. Cao, W.; Zhou, Y.; Güneralp, B.; Li, X.; Zhao, K.; Zhang, H. Increasing global urban exposure to flooding: An analysis of long-term annual dynamics. *Sci. Total Environ.* **2022**, *817*, 153012. [CrossRef] [PubMed]

46. Ahmed, F.; Moors, E.; Khan, M.S.A.; Warner, J.; Van Scheltinga, C.T. Tipping points in adaptation to urban flooding under climate change and urban growth: The case of the Dhaka megacity. *Land Use Policy* **2018**, *79*, 496–506. [CrossRef]